On the synthesis and magnetic properties of multiwall carbon nanotube–superparamagnetic iron oxide nanoparticle nanocomposites

2009 Nanotechnology 20 055607

(http://iopscience.iop.org/0957-4484/20/5/055607)

Nanotechnology **20** (2009) 055607 (7pp) doi:10.1088/0957-4484/20/5/055607

On the synthesis and magnetic properties of multiwall carbon nanotube–superparamagnetic iron oxide nanoparticle nanocomposites

T N Narayanan[1], A P Reena Mary[1], M M Shaijumon[2], Lijie Ci[2], P M Ajayan[2,3] and M R Anantharaman[1,3]

[1] Department of Physics, Cochin University of Science and Technology, Cochin-22, Kerala, India
[2] Department of Mechanical Engineering and Materials Science, Rice University, Houston, TX, USA

E-mail: ajayan@rice.edu and mraiyer@yahoo.com

Received 8 August 2008, in final form 15 October 2008
Published 12 January 2009
Online at stacks.iop.org/Nano/20/055607

Abstract

Multiwall carbon nanotubes (MWCNTs) possessing an average inner diameter of 150 nm were synthesized by template assisted chemical vapor deposition over an alumina template. Aqueous ferrofluid based on superparamagnetic iron oxide nanoparticles (SPIONs) was prepared by a controlled co-precipitation technique, and this ferrofluid was used to fill the MWCNTs by nanocapillarity. The filling of nanotubes with iron oxide nanoparticles was confirmed by electron microscopy. Selected area electron diffraction indicated the presence of iron oxide and graphitic carbon from MWCNTs. The magnetic phase transition during cooling of the MWCNT–SPION composite was investigated by low temperature magnetization studies and zero field cooled (ZFC) and field cooled experiments. The ZFC curve exhibited a blocking at ∼110 K. A peculiar ferromagnetic ordering exhibited by the MWCNT–SPION composite above room temperature is because of the ferromagnetic interaction emanating from the clustering of superparamagnetic particles in the constrained volume of an MWCNT. This kind of MWCNT–SPION composite can be envisaged as a good agent for various biomedical applications.

(Some figures in this article are in colour only in the electronic version)

1. Introduction

The landmark paper on carbon nanotubes (CNTs) by Iijima [1] in 1991 and the subsequent successful synthesis of CNTs in bulk [2] triggered a multitude of research activities on CNT based materials. CNTs and CNT based materials are appealing to both engineers and scientists because of their superlative physicochemical properties [3–7]. CNTs display excellent electrical, thermal and mechanical properties [8] which are highly desirable for various applications. CNTs assume significance not only because of their unique electrical and optical properties but also because they are ideal templates for the synthesis of various other nanostructures.

The filling of CNTs was accepted as an ingenious idea right from the early days of CNT research [9–14], and attempts at complete filling of CNTs are an ongoing research activity, rewarded with only partial success [15]. The confined existence of particles inside CNTs might introduce interesting new properties which have not been seen in these systems previously [16]. Moreover, the filling of CNTs leads to the confinement of particles, and the confinement of nanoparticles leads to possible quantum mechanical effects. Various chemical [17] and physical methods [18] are in vogue for filling CNTs. Immediately after the theoretical prediction of

[3] Authors to whom any correspondence should be addressed.

capillary filling of CNTs by Pederson and Broughton [19], attempts were made to fill CNTs by capillary action of molten metals. However, attempts to completely fill CNTs were in vain or have met with only partial success [20].

Nanocapillarity is the spontaneous penetration of fluids into wettable capillaries, and it can be effectively utilized for filling large area of CNTs [15]. This technique received the much needed fillip when open ended aligned CNTs were prepared [21]. Potential applications of filled CNTs with different materials are in areas such as nanofluidic devices and functional devices like nanoexplorers and cell manipulators. The lack of complete understanding of liquid flow through nanochannels has propelled further activities on the filling of CNTs by capillarity and their further characterizations [22, 23]. It must be noted here that the melting of materials often results in loss of useful physical properties of materials. Filling of CNTs with colloidal suspensions was thought of as an alternative to the filling of CNTs with molten materials.

Ferrofluids (FFs) are colloidal suspensions of magnetic particles and they display novel magnetic and magneto-optical properties. The condition for arresting both agglomeration arising out of magnetic dipolar interaction and sedimentation due to gravity necessitates the size of magnetic particles inside the suspension to be less than 10 nm [24]. These nanometer sized magnetic particles in an FF are to be coated with an organic hull, thus preventing them from agglomeration. The size constraint leads to interesting applications for FFs under the action of an applied magnetic field. FFs can either be synthesized using hydrocarbon carriers or they can be aqueous based. Hydrocarbon based FFs are noted for their extensive applications in various engineering fields [25]. The magneto-optical and viscous properties of these FFs are utilized in making devices like heat sinks, damping arrestors and optical switches, and they can be used as magnetic inks in high speed printing technology [26]. Aqueous magnetic fluids find innumerable applications in therapy, diagnostics and as nanoprobes for biological applications [27].

The absence of any natural magnetic ordering in CNTs and the growing demand for structured nanomagnets in fields such as NEMS (nanoelectro-mechanical systems) [15], medicine and in defense encouraged hybridization of CNTs with magnetic materials. The use of ferromagnetic (FM) melts to fill CNTs is not practical because of the high melting point of FM metals and the interaction between their melts and carbon [20]. Attempts to fill CNTs with magnetic oxides (ferrites) by employing physical methods such as vigorous stirring with salts [28] and other chemical means did not realize desired objectives. This persuaded researchers to seek alternatives, and filling MWCNTs with FFs was proposed as a viable alternative. Fabrication of CNT–FM composites can be achieved if FM particles can be dispersed as colloidal suspensions in a carrier fluid. Fortunately, FFs offer this platform and they can be effectively utilized for this purpose.

In addition to a plethora of applications that can be perceived with FF filled CNTs, they are ideal templates for investigating the magnetic properties at the fundamental level. Confinement of ultrafine magnetic particles will give rise to volume effects and will induce shape anisotropy. The complex interplay between various interactions like exchange interaction, dipolar interaction and shape anisotropy along with various other surface effects will provide a unique opportunity to probe these interactions from a fundamental perspective. FFs are interesting because of the possibility of manipulating the interparticle interaction via dilution. For example, it would be interesting to explore the phenomena of confinement of superparamagnetic iron oxide nanoparticles (SPIONs) inside MWCNTs. When SPIONs are spatially confined inside MWCNTs, various interactions, namely dipolar interaction, exchange interaction, and Ruderman–Kittel–Kasuya–Yosida (RKKY) interaction, determine the overall magnetic property of the composite. It is in this context that a systematic investigation on the filling of MWCNTs with SPIONs becomes an attractive proposition. This is one of the objectives of the present study. Emphasis is laid in synthesizing both MWCNTs and SPION based FFs. These precharacterized MWCNTs and FFs are employed for preparing composites based on a CNT–SPION composite. It has been mentioned earlier that FF filled CNTs can serve as potential nanoprobes for biological applications and as agents for magnetic hyperthermia. CNTs as well as SPIONs are biocompatible and hence so is the combination of both. The ease with which CNTs can be functionalized provides further leverage to target CNTs to a specific site by the application of an external magnetic field. So yet another motivation of the present study is to explore these possibilities by the synthesis of a CNT–SPION composite.

With these objectives in mind, MWCNT–SPION composites were prepared by employing the nanocapillarity of FFs in MWCNTs. The magnetic properties are evaluated and correlated.

2. Experimental details

2.1. Synthesis of MWCNTs

MWCNTs were synthesized by template assisted chemical vapor deposition (CVD) over a nanoporous alumina template (Whattman). Acetylene was used as the precursor for pyrolysis. The flow rate and the deposition rate of acetylene were optimized during the CVD process to obtain MWCNTs with maximum inner diameter. This resulted in open ended nanotubes which were then plasma etched to remove the amorphous carbon present.

2.2. Synthesis of aqueous FFs (AFFs)

AFFs were synthesized by a controlled co-precipitation technique. Initially, nanosized iron oxide particles were prepared by a chemical co-precipitation method with ferric chloride ($FeCl_3$) and ferrous sulfate ($FeSO_4{\cdot}7H_2O$) in the molar ratio 2:1. Aqueous ammonia was added to this solution aided by constant stirring at room temperature, maintaining the pH at 10. The resultant blackish iron oxide precipitate was collected and dispersed in a 3 M citric acid solution. The resultant mixture was maintained at 90 °C for half an hour and the residue was collected and dispersed in water by extensive sonication. By this technique, highly viscous ferrofluids with high shelf life and high thermal stability could be prepared.

2.3. Synthesis of MWCNT–SPION composite

For the synthesis of MWCNT–SPION composite, one drop of AFF (∼3 μl) was placed over MWCNTs. The fluid infiltrated in to the nanotubes instantaneously. A magnetic field ($\mu_0 H \sim$ 1 T) was applied along the tube axis to enhance the infiltration process.

The carrier fluid was evaporated off at room temperature. Subsequently, the CNTs were etched by sonicating with ethanol in order to remove the surface layer. The alumina template was removed (for certain studies such as scanning electron microscopy (SEM), transmission electron microscopy (TEM), and energy dispersive spectroscopy (EDS)) by dissolving the template in a 3 M sodium hydroxide (NaOH) solution, and the residue was magnetically separated.

The morphology of the MWCNT–SPION composite was studied using field emission scanning electron microscopy (FESEM: JSM-6335 FESEM). The room temperature and low temperature magnetic properties of the CNT–SPION composite were investigated using a SQUID magnetometer (MPMS-5S XL, Quantum Design). transmission electron microscopy (TEM) experiments were performed using a JEM 2010 transmission electron microscope. SQUID measurements were carried out by keeping the MWCNT–SPION composite inside the alumina template in order to have the alignment intact.

3. Results and discussion

The AFF prepared by co-precipitation exhibited high thermal stability and offered high shelf life. The fluid spiked even under small applied magnetic fields, and this is an indicator of the fact that the FF synthesized by this method was of high quality. Figure 1 shows the schematic of the infiltration processes.

Figure 2(a) shows an FESEM image of AFF filled MWCNTs after the removal of the alumina template. The microRaman spectrum of MWCNTs with an excitation wavelength at 514 nm is shown in figure 2(b). The spectrum is characteristic of the order G (1600 cm^{-1}) and the disorder D (1330 cm^{-1}) peaks exhibited by graphite. The energy dispersive spectrum of the MWCNT–SPION composite is displayed in figure 2(c). Evidence for the presence of the element iron emanating from iron oxide can be clearly seen in the spectrum.

The TEM characterization was carried out after removing the alumina template using 3 M NaOH, and the residue was magnetically separated. Two sets of samples were prepared for TEM analysis (in order to verify the filling of SPION particles inside MWCNTs) by dispersing the residue in ethanol and sonicating the residue for few minutes. This solution was drop cast over a TEM copper grid. TEM images derived from two different parts (figures 3(a) and (b)) of the sample reveal filling of CNTs with FF. The average size of the SPIONs is found to be ∼12 nm (figure 3(c)). It is also evident from figures 3(a) and (b) that there is no SPION residing in between the MWCNTs. The selected area electron diffraction (SAED) images (figure 3(d)) are indicative of the superimposition of several planes. They correspond to polycrystalline planes of graphite, (110) and (112), and nanocrystalline planes from iron oxide, (440).

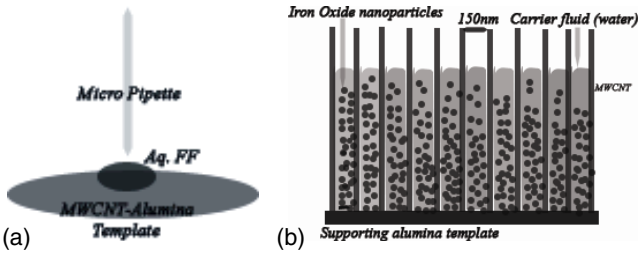

Figure 1. Schematic illustration of MWCNT filling by AFF. (a) Infiltration, (b) AFF filled MWCNT.

The size distribution of SPIONs is depicted in figure 4. The distribution is Gaussian and is centered at ∼11.7 nm.

3.1. Magnetic studies

The room temperature hysteresis loop of the composite is shown in figure 5. The hysteresis loop is typical of a superparamagnetic material with near-zero coercivity (H_c) and negligible remanence (M_r).

Fitting the Langevin function with the experimentally observed M–H curve is considered as a sure test for superparamagnetism (SPM).

The Langevin function can be written as

$$L(x) = \coth x - \frac{1}{x}. \tag{1}$$

However, if due weightage is not given to the size distribution, this fitting can be erroneous and can be misleading. So, after providing due weightage for the size distribution, the Langevin function is modified as [29]

$$L(x) = 1/2bx \int_{x(1-b)}^{x(1+b)} L(x')\,\mathrm{d}x' \tag{2}$$

$$= 1/2bx \ln\left\{\frac{(1-b)\sinh[x(1+b)]}{(1+b)\sinh[x(1-b)]}\right\} \tag{3}$$

where b is the width of the size distribution. This modified function in equation (3) was used to simulate the magnetization curve, and is shown in figure 6.

The function fit is in agreement, and it reaffirms the fact that the MWCNT–SPION composite exhibits SPM. It is to be noted here that the magnetic response of AFF filled MWCNT originates from the SPIONs.

A better understanding of these spatially constrained SPION particles can be arrived at by a temperature dependent magnetization study. The magnetization of the CNT–SPION composite was recorded at 6 K and is depicted in figure 7. It is noteworthy that it exhibited enhanced coercivity (∼150 Oe) and nonzero remanence.

In order to probe the magnetic phase transitions emerging at low temperatures, zero field cooling–field cooling (ZFC–FC) measurements were carried out under an applied magnetic field of 300 Oe. The results are shown in figure 8.

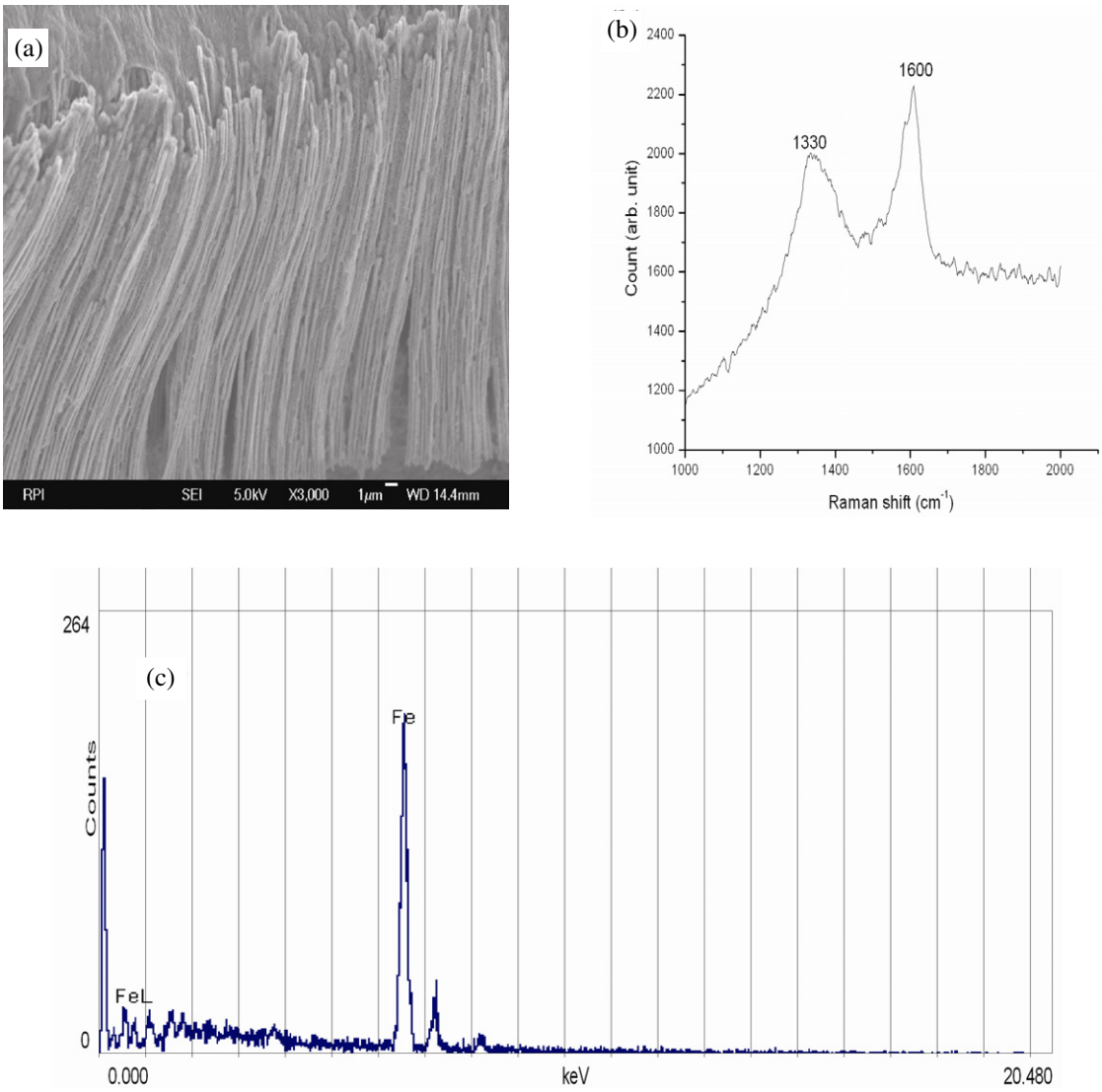

Figure 2. (a) FESEM image, (b) microRaman spectrum, and (c) EDS spectrum of AFF filled MWCNTs.

The ZFC curve shows a blocking behavior [30] at ∼110 K. The blocking temperature T_B is related to the size of the superparamagnetic particles by the relation [31]

$$KV = 25k_BT \tag{4}$$

where k_BT is the thermal energy, K the anisotropy constant (for magnetite 1.35×10^4 J m^{-3}), and V the volume of the particle. The blocking temperature T_B calculated for 12 nm magnetite particles is ∼40 K. The deviation can be attributed to the clustering of SPION particles [32]. The TEM images (figures 3(a) and (b)) also provide proof for clustering of SPION particles within MWCNTs.

This implies that magnetic properties of an ensemble of single domain particles follows that of single particles and that the particle–particle interaction is not strong enough to prevent the collective behavior of the system at these temperatures.

It is to be noted here that the FC and ZFC measurements carried out on these samples exhibit an anomaly near room temperature. Above room temperature they show a ferromagnetic like behavior up to 400 K. Here, ZFC measurements were carried out by cooling the sample in zero field up to 6 K and then the moment is measured while warming in a field of 300 Oe. In FC measurements, the sample is cooled in a field of 300 Oe up to 6 K and the moment is evaluated while warming up to a temperature ∼400 K. The ground states of ZFC and FC are different and a similar variation in ZFC and FC measurements above room temperature indicates that the transition is reversible and intrinsic. This observation points to the fact that there is a ferromagnetic like moment ordering due to possible exchange interaction taking place between constrained superparamagnetic particles.

Figure 9 shows the ZFC–FC curve for bare MWCNTs. The ZFC–FC curves do not show any magnetic phase transition, indicating that the anomalous transition undergone in the case of the MWCNT–SPION composite (figure 8) does not emanate from the MWCNTs.

It is known that magnetic relaxation and blocking play a major role in fine particle systems when they are randomly oriented [30]. Once the temperature is increased above

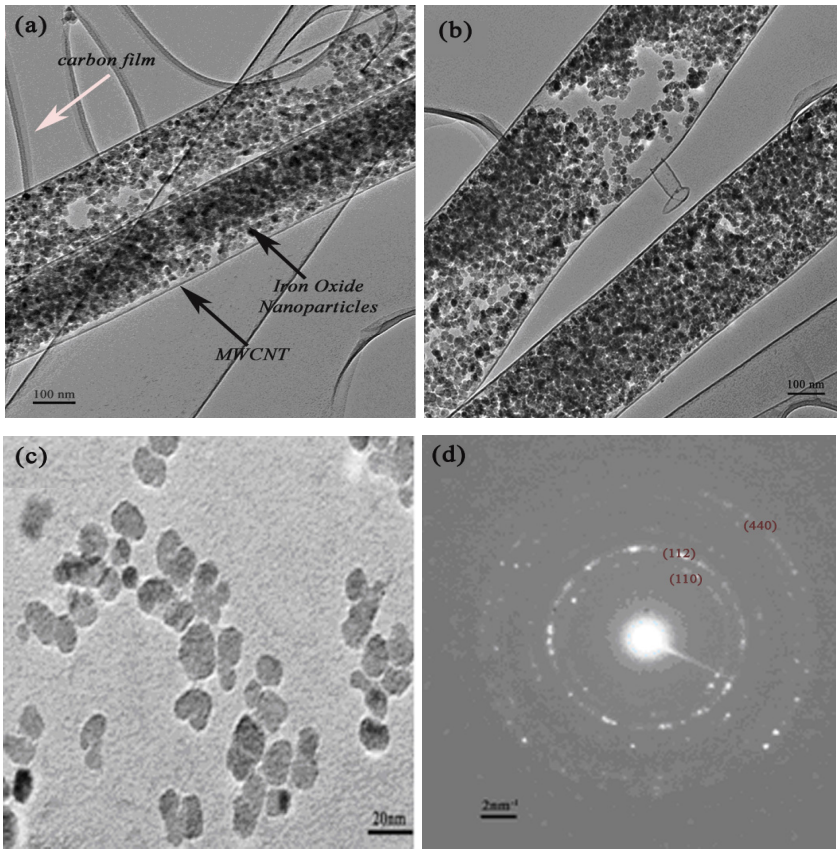

Figure 3. (a), (b) TEM images of AFF filled MWCNTs, (c) TEM image of the AFF of the SPIONs, (d) selected area electron diffraction (SAED) image of an AFF filled MWCNT.

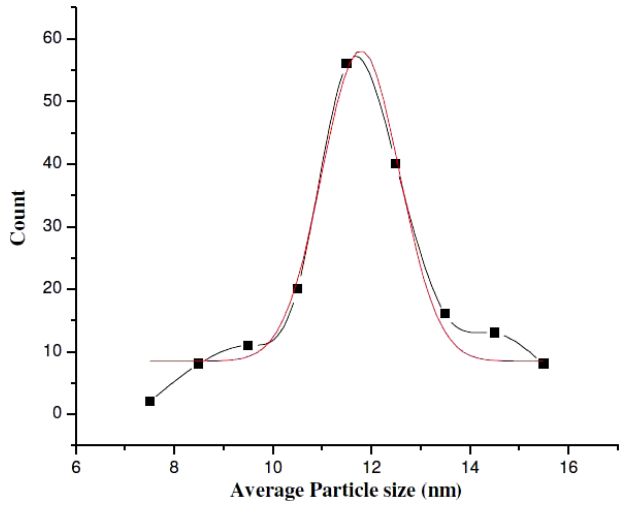

Figure 4. Particle size distribution from TEM observation.

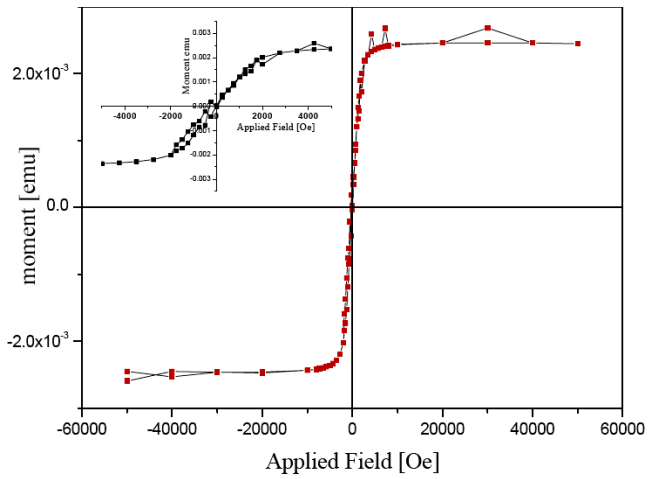

Figure 5. $M(H)$ curve for MWCNT–SPION composite at room temperature.

room temperature, thermal energy wins over the electrostatic polar repulsive energy between each nanoparticle, which stops the particles from agglomeration in the case of a ferrofluid. However, when the nanoparticles are constrained to small volumes, the role of interparticle interaction cannot be ignored and this may initiate an exchange interaction between the nanoparticles. However, this warrants a detailed investigation, which is in progress.

4. Conclusions

MWCNT–SPION composites were prepared by employing the nanocapillarity of ferrofluids. Magnetization studies of MWCNT–SPION composites conducted at room temperature and low temperature suggest that the embedded iron oxide nanoparticles exclusively contribute to the magnetic properties

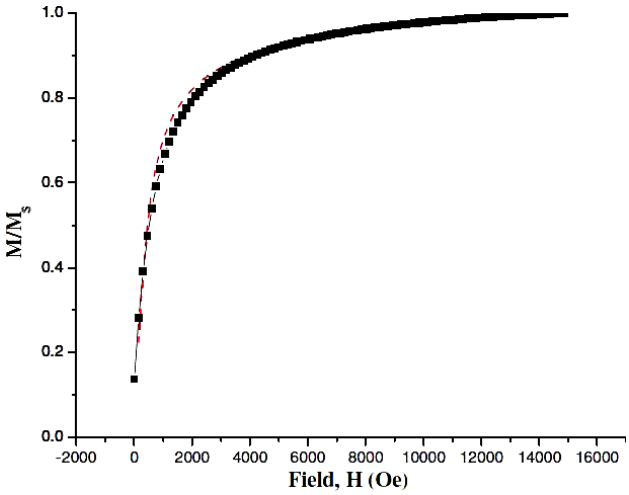

Figure 6. Langevin function fit (dotted line) to the experimental curve.

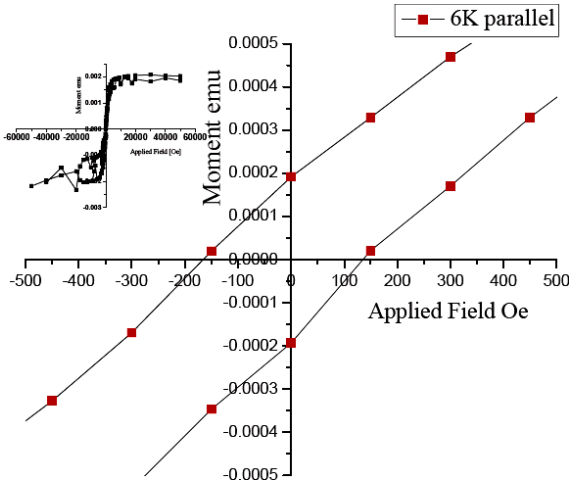

Figure 7. $M(H)$ curve for MWCNT–SPION composite at 6 K.

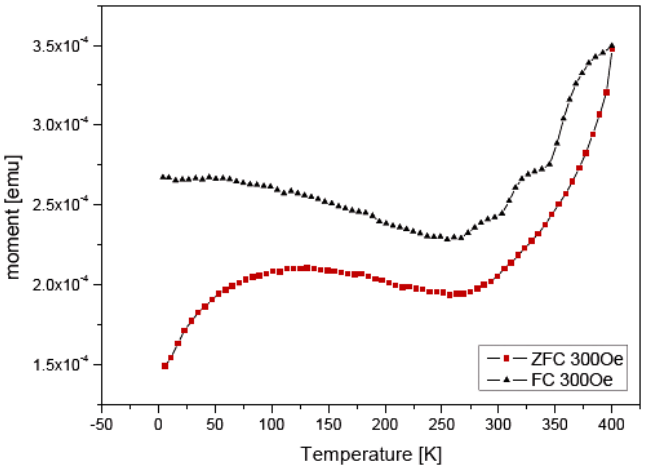

Figure 8. ZFC–FC curves for MWCNT–SPION composite.

of the composite. The anomalous FM like behavior exhibited by this system above room temperature is probably due to the enhanced interparticle exchange interaction. This kind of

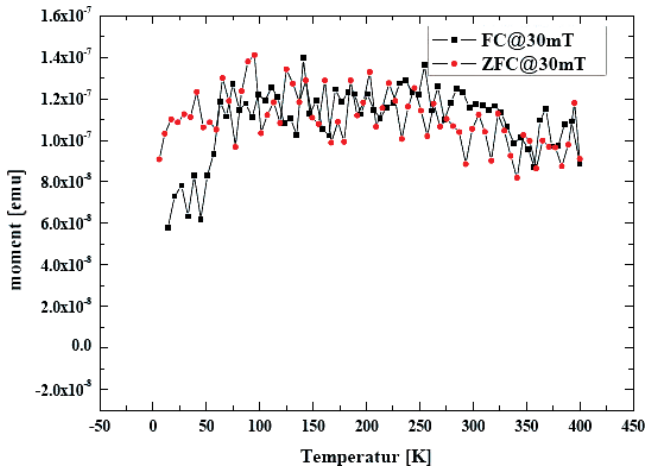

Figure 9. ZFC–FC curves for MWCNTs.

MWCNT–SPION composite can be envisaged as a good agent for drug delivery and can be easily navigated through blood stream with augmented heating for hyperthermia.

Acknowledgments

TNN acknowledges the financial support received from Interconnect Focus Center at Rensselaer Polytechnic Institute, Troy, New York, USA. TNN thanks KSCSTE (D.O.No.004/FSHIP/05/KSCSTE), Kerala, India and RMAP thanks CSIR (F.NO.9/239(379)/2004-EMR-1) for financial support in the form of fellowships. TNN and MRA acknowledge Professor Gunter Schatz, Professor Manfred Albrecht, Dr Sebastian Fischer and Dr Ildico Guhr, Department of Physics, University of Konstanz, for SQUID measurements and fruitful discussions. MRA thanks DST-DAAD PPP (INT/DAAD/P-152/2006) for awarding an exchange program.

References

[1] Iijima S 1991 *Nature* **354** 56–8
[2] Ebbesen T W and Ajayan P M 1992 *Nature* **358** 220–1
[3] Baughman R H, Zakhidov A A and de Heer W A 2002 *Science* **297** 787–92
[4] Rossi M P, Ye H H, Gogotsi Y, Babu S, Ndunga P and Bradley J C 2004 *Nano Lett.* **4** 989–93
[5] Tolles W M and Rath B B 2003 *Curr. Sci.* **85** 1746–59
[6] Gogotsi Y 2003 *Mater. Res. Innov.* **7** 192–4
[7] Lin Y, Taylor S, Li H P, Fernando K A S, Qu L W, Wang W, Gu L, Zhou B and Sun Y P 2004 *J. Mater. Chem.* **14** 527–41
[8] Dresselhaus M S, Dresselhaus G and Jorio A 2004 *Annu. Rev. Mater. Res.* **34** 247–78
[9] Terrones M, Grobert N, Hsu W K, Zhu Y Q, Hou W B, Terrones H, Hare J P, Kroto H W and Walton D R M 1999 *Mater. Res. Soc. Bull.* **24** 43–9
[10] Monthioux M 2002 *Carbon* **40** 1809–23
[11] Ajayan P M 1997 *Prog. Cryst. Growth Charact. Mater.* **34** 37–51
[12] Rao C N R, Sen R and Govindaraj A 1996 *Solid State Mater. Sci.* **1** 279–84
[13] Ajayan P M, Stephan O, Redlich Ph and Colliex C 1995 *Nature* **375** 564–5
[14] Ajayan P M and Iijima S 1993 *Nature* **361** 333–4

[15] Seifu D, Hijji Y, Hirsch G and Karna S P 2008 *J. Magn. Magn. Mater.* **320** 312–5
[16] Tyagi P K, Singh M K and Misra D S 2002 *Encyclopedia of Nanoscience and Nanotechnology* vol 3, ed H S Nalwa (New York: American Scientific Publishers) pp 417–30
[17] Tsang S C, Chen Y K, Harris P J F and Green M L 1994 *Nature* **372** 159–62
[18] Vasilios G, Vasilios T, Dimitrios G and Dimitrios P 2005 *Chem. Mater.* **17** 1613–7
[19] Pederson M R and Broughton J Q 1992 *Phys. Rev. Lett.* **69** 2689–92
[20] Korneva G, Ye H, Gogotsi Y, Halverson D, Friedman G, Bradley J C and Konstantin G K 2005 *Nano Lett.* **5** 879–84
[21] Choi Y C, Shin Y M, Lee B S, Park G S, Choi W B, Lee N S and Kim J M 2000 *Appl. Phys. Lett.* **76** 2367–9
[22] Werder T, Walther J H, Jaffe R L, Halicioglu T, Noca F and Koumoutsakos P 2001 *Nano Lett.* **1** 697–702
[23] Kim B M, Sinha S and Babu H H 2004 *Nano Lett.* **4** 2203–8
[24] Rosenweig R E 1985 *Ferrohydrodynamics* (Cambridge: Cambridge University Press) pp 33–60
[25] Popplewell J 1984 *Phys. Technol.* **15** 150–6
[26] Nair S S, Thomas J, Sandeep C S S, Anantharaman M R and Philip R 2008 *Appl. Phys. Lett.* **92** 171908
[27] Bryant H C, Sergatskov D A, Lovato D, Adolpji N L, Larson R S and Flynn E R 2007 *Phys. Med. Biol.* **52** 4009–25
[28] Gao X P, Zhang Y, Chen X, Pan G L, Yan J, Wu F, Yuan H T and Song D Y 2004 *Carbon* **42** 47–52
[29] Chikazumi S 1964 *Physics of Magnetism* (New York: Wiley) pp 411–2
[30] Battle X and Labarta A 2002 *J. Phys. D: Appl. Phys.* **35** R15–42
[31] Cullity B D 1972 *Introduction to Magnetic Materials* (*Addison-Wesley Series in Metallurgy and Materials*) (Reading, MA: Addison-Wesley) pp 410–8
[32] Poddar P, Wilson J L, Srikanth H, Morrison S A and Carpenter E E 2004 *Nanotechnology* **15** S570–4